*Proc. Natl. Acad. Sci. USA*
Vol. 96, pp. 5141–5146, April 1999
Immunology

# Murine natural killer cells contribute to the granulomatous reaction caused by mycobacterial cell walls

I. Apostolou*, Y. Takahama†, C. Belmant‡, T. Kawano§, M. Huerre¶, G. Marchal‖, J. Cui§, M. Taniguchi§, H. Nakauchi**, J.-J. Fournié‡, P. Kourilsky*, and G. Gachelin*††

*Unité de Biologie Moléculaire du Gène, Institut National de la Santé et de la Recherche Médicale U277, ¶Unité d'Histopathologie, and ‖Unité de Physiopathologie de l'infection, Institut Pasteur, 25 rue du Dr. Roux, 75724 Paris Cedex 15, France; †Precursory Research for Embryonic Science and Technology (Japan Science and Technology Corporation) and **Core Research for Evolutional Science and Technology (Japan Science and Technology Corporation), Department of Immunology, Institute of Basic Medical Sciences, Tsukuba University, Tsukuba 305, Japan; ‡Institut National de la Santé et de la Recherche Médicale U395, Centre Hospitalier Universitaire Purpan, Toulouse, France; and §School of Medicine, Chiba University, Chiba 260, Japan

*Communicated by William E. Paul, National Institute of Allergy and Infectious Diseases, Bethesda, MD, March 3, 1999 (received for review November 25, 1998)*

**ABSTRACT** **Mice injected with deproteinized cell walls prepared from the strain H37rv of *Mycobacterium tuberculosis* develop a granuloma-like lesion in which NKT cells are predominant. NKT cells play a primary role in the granulomatous response, because the latter does not occur in J$\alpha$281$^{-/-}$ mice, which miss NKT cells. The glycolipidic fraction of the cell walls is responsible for the recruitment of NKT cells; the recruiting activity is associated with fractions containing phosphatidylinositolmannosides. These results define a powerful experimental set up for studying the *in vivo* induction of NKT cell responses to microbial components.**

Murine natural killer (NKT) cells are $\alpha/\beta$ T lymphocytes expressing NK-associated cell surface markers such as NK1.1 (1) and some members of the Ly-49 family (2). They differ from conventional T lymphocytes by several other features: they use an invariant T cell antigen receptor $\alpha$ (TCR$\alpha$) chain consisting in rearranged V$\alpha$14 and J$\alpha$281 segments and a conserved complementary determining region 3 (CDR3) (3, 4); their TCR$\beta$ repertoire is mostly skewed toward the usage of V$\beta$8 and V$\beta$7 segments (reviewed in ref. 5); they express TCR at an intermediate level and are restricted by the MHC class Ib molecule, CD1d (reviewed in ref. 5). The $\alpha$1 and $\alpha$2 domains of the CD1d1 molecule fold into a groove that accommodates the lipidic moiety of glycosylceramides (6) or glycosylphosphatidylinositol (GPI)-anchored proteins, yielding the CD1–glycolipid complexes recognized by NKT cells (6–10).

The *in vivo* functions of NKT cells are not described fully. They are involved in the IgG response to the GPI-anchored proteins of *Plasmodium* and *Trypanosoma* (10). They contribute to the IL-12-mediated rejection of tumors (11–13). They are also involved in some autoimmune diseases and infectious processes, through the production of T helper (Th)-1- or Th-2-type cytokines (14–16) or through an impairment in their cell number (17–20). Nevertheless, the mechanisms that initiate the *in vivo* activation of NKT cells in these responses are unknown. The identification of molecules involved in their *in vivo* activation or recruitment thus should contribute to a better understanding of the functions of NKT cells.

We have designed an *in vivo* experimental set-up in which NKT cells are recruited locally. The s.c. injection of mice with deproteinized mycobacterial cell walls results in the development of a granuloma-like lesion in which NKT cells predominate among $\alpha/\beta$ T cells. More importantly, NKT cells, the accumulation of which is driven by mycobacterial oligomannosylated GPI, play an active role in the formation of the lesions. The present experimental design provides a powerful tool for studying *in vivo* the responses of NKT cells to nonpeptidic microbial antigens and other glycolipids.

## MATERIALS AND METHODS

**Animals.** The animals were: C57BL/6, C57BL/6 MHC class II$^{-/-}$ (21), C57BL/6 $\beta_2$-microglobulin ($\beta_2$m)$^{-/-}$ (22), J$\alpha$281$^{-/-}$ (12), and J$\alpha$281$^{+/-}$ mice. The latter two were backcrossed, respectively, nine and six times from the 129/Sv− onto the C57BL/6 background. Mice were kept in biohazard safety facilities and handled in compliance with the rules of the French Ministry of Agriculture and Fisheries.

**Bacterial Strains and Extracts.** *Mycobacterium tuberculosis* bacilli (strain H37Rv) were grown on a semisolid medium and heat-killed (75°C, 30 min). After sonic disruption in $10^{-2}$ M Tris, pH 8.0/$10^{-3}$ M $MgCl_2$/$10^{-3}$ M $CaCl_2$/1.5 $\times$ $10^{-1}$ M NaCl, the extracts were digested for 5 hr at 37°C with 25 $\mu$g/ml of DNase and RNase, followed by heat inactivation. After washes, the suspension was incubated for 24 hr at 37°C with trypsin, chymotrypsin, and subtilisin (Boehringer Mannheim) at a final concentration of 200 $\mu$g/ml each in the same buffer, supplemented by 0.5% SDS. After heat activation (10 min, 70°C), the particles were washed and resuspended in PBS. The absence of proteins was monitored by PAGE and amino acid analysis. Samples were standardized on the basis of their sugar content.

Lipids were extracted and fractionated as follows. Four grams of bacilli were extracted twice with $CHCl_3/CH_3OH$ (1:1, vol/vol). The extracts were pooled, dried, suspended in $CHCl_3/H_2O$, and left for 1 hr at 4°C for partition between the organic phase of crude lipids (fraction I) and the aqueous phase (including lipido arabino mannan, polysaccharides, and denatured proteins at the interface) (fraction II). Fraction I, devoid of the phosphoantigens able to activate $\gamma/\delta$ T cells in humans (23), was dried and fractionated by cold (10°C) acetone extraction, resulting in a soluble extract (fats, phenolic glycolipids) and an insoluble white precipitate. Hot acetone (50–60°C) was added to the waxy pellet, extracting mycolyl trehalose antigens and other glycolipids (fraction III) while precipitating total phosphatidylinositolmannosides (PIMs) and lipooligosaccharides (LOS) (fraction IV). Fraction IV was dried and split by methanol solubilization into total PIMs

Abbreviations: PIM, phosphatidylinositolmannoside; CDR3, complementary determining region 3; GPI, glycosylphosphatidylinositol; NKT, natural killer T; TCR, T cell antigen receptor; PE, phycoerythrin; $\beta_2$m, $\beta_2$-microglobulin; Alu-Gel-S, aluminium hydroxide.

††To whom reprint requests should be addressed at: Unité de Biologie Moléculaire du Gène, Département d'Immunologie, Institut Pasteur, 25 rue du Dr. Roux, 75724 Paris Cedex 15, France. e-mail: ggachel@pasteur.fr.

The publication costs of this article were defrayed in part by page charge payment. This article must therefore be hereby marked "*advertisement*" in accordance with 18 U.S.C. §1734 solely to indicate this fact.

PNAS is available online at www.pnas.org.

(white pellet, fraction V) and soluble LOS (fraction VI). Polar PIMs precipitated on cooling fraction III, yielding fraction VII. All fractions were analyzed by TLC on silicic acid pF254 (Merck) with $CHCl_3/CH_3OH/H_2O$, 60:35:5, and by using *M. tuberculosis* $PIM_2$ as standard. The spots were revealed by using sulfuric-anthrone spray.

**PCR Primers.** Vβ-specific primers have been described elsewhere (24, 25). The Cβ-specific primer was GCCCATGGAACTGCACTTGGC. The labeled Cβ-specific primer was FAM-CTTGGGTGGAGTCACATTTCTC. Concerning primers for $V\alpha14^+$ cDNAs, Vα14-specific primer was CTAAGCACAGCACGCTGCACA, Cα primer was TGGCGTTGGTCTC TTTGAAG, and the labeled Cα primer was FAM-ACACAGCAGGTTCTGGGTTC; the Jα281-specific primer was CAGGTATGACAATCAGCTGAGTCC and the labeled Jα281-specific primer was FAM-CAGCTGAGTCCCAGCTCC. The labeled NKT clonotypic primer was FAM-GCTGAACCTCTATCNCCCACC. The CD4-specific 5′ primer was CTGAATTCGGCGCTTGCTGCTGC, and the 3′ primers were CACAAGCTTAAGTCTGAGAGTCTTCC and FAM-TGCTGATTCCCCTTCCTTCC. The CD8-specific 5′ primer was TAGAATCCTAGCTTGACCTAAGC, and the 3′ primers were ATGGATCCATATAGACAACGAAGG and FAM-GGATAATCGACTCACCC. The primers for HPRT were 5′ primer GTAATGATCAGTCAACGGGGGAC and 3′ primers CCAGCAAGCTTGCAACCTTAACCA and FAM-TTCTTTCCAGTTAAAGTTG. The primers for CD3ε were 5′ primer GCCTCAGAAGCATGATAAGC and 3′-FAM-CCCAGAGTGATACAGATGTC. The primers for IgM heavy chains were FAM-TTCAGTGTTGTTCTGGTAG, 3′ primer CTGGATCCGGCACATGCAGATCTC, and 5′ primer AGTCCTTCCCAAATGTCTTCCC. The unlabeled Vγ1-, Cγ-, Vδ2-, Vδ4-, Vδ5-, Vδ6-, and Cδ-specific primers were as in ref. 26. The Vδ1- and Vδ6P-specific primers were ATTCAGAAGGCAACAATGAAAG and CTGTAGTCTTCCAGAAATCAC, respectively; the labeled Cδ-specific primer was FAM-TTTCACCAGACAAGCAACA; the Vγ2- and Vγ7-specific primers were CGGCAAAAAACAAATCAACA and CTATAACTTCGTCAGTTCCAC, respectively; the labeled Vγ primer specific for the Vγ1 and Vγ2 segments was FAM-CCTCCTAAGGGTCGTTGATT, and the labeled Vγ7-specific primer was FAM-CTTGTCCGGGCCTTCAT.

**Semiautomated ("Immunoscope") Analysis of T Cell Diversity.** The technique has been described elsewhere (27–29). Briefly, total RNA was extracted and 10 μg was reverse-transcribed by using avian myeloblastosis virus reverse transcriptase (RT). The quality and quantity of the resulting cDNA (final volume of 100 μl) were monitored by assaying hypoxanthine phosphoribosyltransferase cDNA. One microliter of the cDNA solution was PCR-amplified through 40 cycles (94°C, 1 min; 60°C, 1 min; 72°C, 4 min) by using either Vα14- and Cα-specific primers or each of the Vβ- and a Cβ-specific primers. Two microliters of the PCR products were used in run-off experiments (5 cycles) by using fluorescent primers specific for Jα281 or Cα segments. The length of the CDR3 region and the intensity of fluorescence of the run off products were determined on an automatic sequencer (Applied Biosystems). The size distribution of the CDR3 region for a V-C couple is depicted as a family of peaks separated by 3 nt (derived from in-frame mRNA), the area of which is proportional to the initial amount of the considered mRNA. In the absence of antigen-driven proliferation, the six to eight peaks observed display a Gaussian-like distribution. An antigen-driven T cell proliferation typically results in distortions to the Gaussian distribution. Semiquantitative PCR was adapted from a published procedure (26) by normalizing on the basis of CD3ε mRNA. Ten thousand T cells were sufficient to perform a semiquantitative PCR analysis of the complete Vβ-Cβ repertoire by using the Immunoscope technique.

**Antibodies and Fluorescence-Activated Cell Sorter (FACS) Analysis.** *Cells.* Granuloma cells were prepared by forcing minced granulomas through a 70-μm nylon cell strainer (Becton Dickinson) and washed once in PBS. Living cells were separated by Ficoll fractionation (Lympholyte-M; Cedarlane Laboratories). Liver leukocytes were obtained by discontinuous Percoll gradient.

*Antibodies.* Biotinylated-anti-Vα14 (clone CMS-5) has been described previously (30). The following reagents were purchased from PharMingen: phycoerythrin (PE)-NK1.1 (clone PK136), FITC- or biotinylated TCRβ (clone H 57–597), FITC-CD4 (clone RM4–5), FITC-CD44 (clone IM7), biotinylated CD45.2 (clone 104), PE-B220 (clone RA3–6B2), FITC-CD19 (clone 1D3), and PE-streptavidin, FITC-, PE-, and biotinylated normal mouse Ig, which were used as negative controls. FITC-CD8 (clone CT-CD8a) was from Caltag (South San Francisco, CA). Allophycocyanin–streptavidin was from Molecular Probes.

**FACS Analysis.** The cells first were incubated with murine serum before addition of the proper combinations of antibodies. Dead cells were gated out by propidium iodide staining. Lymphoid cells were gated on FCS and SSC, and a minimum of 100,000 events were counted in the lymphocyte gate. Four-color analysis was carried out by using a FACS-Vantage (Becton Dickinson); three-color analysis was carried out by using a FACScan (Becton Dickinson). Data were analyzed by using CELL-QUEST software (Becton Dickinson). Liver NKT cells were sorted out after labeling with anti-NK1.1 and anti-TCRβ antibodies by using a $FACStar^+$ Becton Dickinson cell sorter.

## RESULTS

The injection of deproteinized mycobacterial cell walls results in the formation of granuloma-like lesions. Because numerous studies have shown that several mycobacterial glycolipids are recognized by human T cells when presented by CD1b, c, and d molecules (31–35) and because similar structural features are attributed to human and mouse NKT cells (6, 9, 36), we first examined whether murine NKT cells could be detected at the site of injection of deproteinized mycobacterial cell walls rich in glycolipids.

Deproteinized mycobacterial cell walls equivalent to $10^6$ *M. tuberculosis* bacilli were injected s.c. at the tail base of C57BL/6 mice. Control animals injected with PBS were sacrificed at days 1, 2, and 3 and, 7 days after injection, showed no sign of an inflammatory process. In immunized mice, neutrophils were predominant on smears prepared from cell infiltrates collected at days 1 and 2. Lymphocytes and macrophages were detected on day 3, and lesions adherent to the skin and the muscles developed thereafter, reaching a diameter of 4–6 mm by day 7. Histological analysis on day 7 lesions showed granuloma-like lesions, with a core rich in neutrophils, surrounded by a rim consisting of a dense array of macrophages, lymphocytes, and fibroblasts (Fig. 1*A*).

**NKT Cells Are the Only $V\alpha14^+$ T Cells That Infiltrate the Granuloma-Like Lesions.** The day 7 granulomas could not be dissociated into live, single-cell suspensions preventing FACS analysis. An RT-PCR-based technique (Immunoscope) (27–29) was used instead to search for mRNAs coding for NKT cell-specific markers. Because a nearly invariant Vα14-Jα281 TCR chain, with a 10-aa-long CDR3, is the signature of the murine NKT cells (4), the Vα14-encoding cDNAs were PCR-amplified and analyzed for their CDR3 diversity by primer extension by using either Cα- or Jα281-specific primers. The Cα-specific primers yielded signals representative of the diversity of $V\alpha14^+$ α-chains in the samples. Several peaks were detected in the lymph nodes draining the site of injection of control and immunized mice (Fig. 1*B*, *a* and *c*). The Gaussian distribution was altered by a predominant peak corresponding

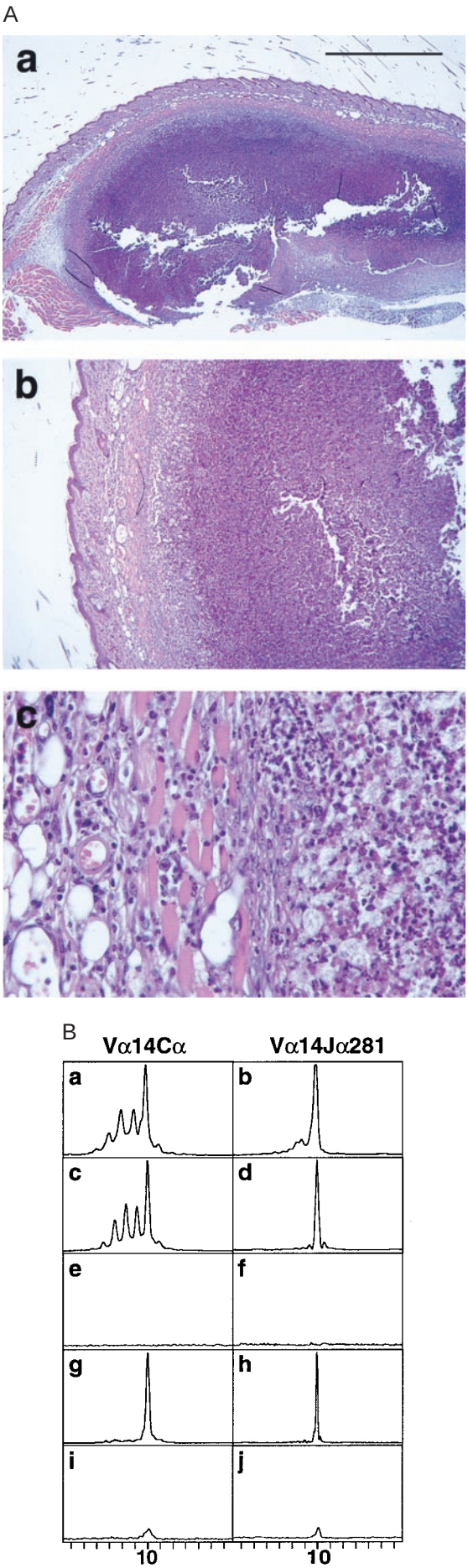


to a CDR3 length of 10 aa and containing Vα14-Jα281-rearranged TCRα chains (Fig. 1*B*, *b* and *d*), thus including NKT cells. No signal was detected in the skin and muscles dissected at the site of PBS injection (Fig. 1*B*, *e* and *f*). In contrast, the Vα14-coding cDNAs prepared from day 7 granuloma-like structures yielded, by using either the Jα- or the Cα-specific primers, a unique peak with a CDR3 size of 10 aa (Fig. 1*B*, *g* and *h*). The direct sequencing of these Vα14-Cα PCR products identified the NKT cell-specific, rearranged α-chains: the 4-nt substitutions at codon 31 accounted for the entire diversity of the Vα14-Jα281 chains of the infiltrating T cells. Thus, unlike lymph node cells, which contain conventional $V\alpha14^+$ T cells, all the $V\alpha14^+$ T cells recruited in day 7 granuloma-like structures are NKT cells. A unique Vα14-Cα peak with a 10-aa-long CDR3 and containing the Jα281 segment was detected in the day 3 cell infiltrates (Fig. 1*B*, *i* and *j*) and was identified further as NKT cell-specific by using a clonotypic probe. Thus, NKT cells are recruited at the earliest stages of the cell infiltration after the injection of mycobacterial cell walls. The same technique allowed the detection of rearranged β-chains by using the Vβ8.1, 7, 3, 5.2, and 10 segments. Rare, conventional $\alpha/\beta$ $CD4^+$ T cells may infiltrate the granuloma-like lesions, because no CD8- and little CD4-encoding mRNAs were detected by using the proper primers. Finally, a PCR survey by using Igμ and γ/δ TCR-specific primers indicated the presence of significant numbers of B cells and γ/δ T cells, particularly those using the Vδ5 and Vδ6 segments (data not shown).

**Involvement of α/β T Cells in the Development of Granuloma-Like Lesions.** Granulomatous responses are multicellular and multistep processes. To approach the possible involvement of α/β T cells in this process, we have immunized mice genetically deficient in several T cell subsets.

$J\alpha281^{-/-}$ mice (12), deficient in NKT cells but in which conventional T cells and NK cells develop normally, were injected with the deproteinized mycobacterial cell walls. In five of seven injected mice, no lesion but, rather, a tiny diffuse infiltrate was detected at the site of injection. In the other two mice, a tiny, structured cell infiltrate nearly exclusively populated by macrophages developed (Fig. 2*A*, *a–d*). Neither Vα14-coding mRNAs (Fig. 2*B*, *a* and *b*) nor VβCβ rearrangements were found in the infiltrates (data not shown). A Gaussian Vα14-Cα profile was obtained from the lymph nodes of the $J\alpha281^{-/-}$ immunized mice, indicating a normal usage of the Vα14 segment by conventional T cells in the absence of NKT cells (Fig. 2*B*, *c* and *d*). IgMμ chains were not detected in the infiltrates, but rearranged TCRγ chains were found. The six $J\alpha281^{+/-}$ mice yielded on immunization the same results as $C57BL/6^{+/+}$ mice (Fig. 2 *A*, *e–g* and *B*, *e–h*). The formation of a highly organized and sizeable granulomatous lesion in response to deproteinized mycobacterial cell walls thus requires the presence of NKT cells.

FIG. 1. (*A*) Hematoxylin/eosin-stained sections of a granuloma-like structure caused by the injection of deproteinized mycobacterial cell walls. C57BL/6 mice were injected s.c. with the equivalent of $10^6$ deproteinized mycobacterial cell walls. At day 7 after the infection, the granuloma-like structures that had developed were excised, fixed in buffered 4% formalin, embedded in paraffin, and sectioned. The objectives used were: 2.5 (*a*), 6.3 (*b*), and 40 (*c*). (Bar = 1 mm.) (*B*) Immunoscope analysis of the Vα14-Cα (*Left*) and Vα14-Jα281 (*Right*) patterns observed 7 days after injection of PBS or deproteinized mycobacterial cell walls to C57BL/6 mice. (*a* and *b*) Lymph nodes of PBS-injected mice. (*c* and *d*) Lymph nodes of mice immunized with deproteinized mycobacterial cell walls. (*e* and *f*) Skin and muscle dissected at the site of PBS injection in control mice. (*g* and *h*) Day 7 granuloma-like structure caused by the injection of deproteinized mycobacterial cell walls. (*i* and *j*) Day 3 cell infiltrate. *x* axis, amino acid length of the CDR3 region. *y* axis, relative intensity of fluorescence.

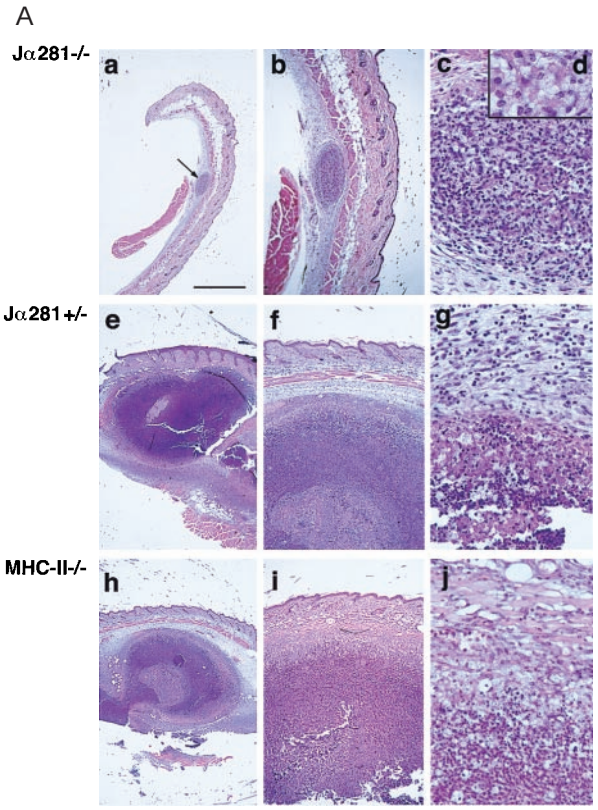


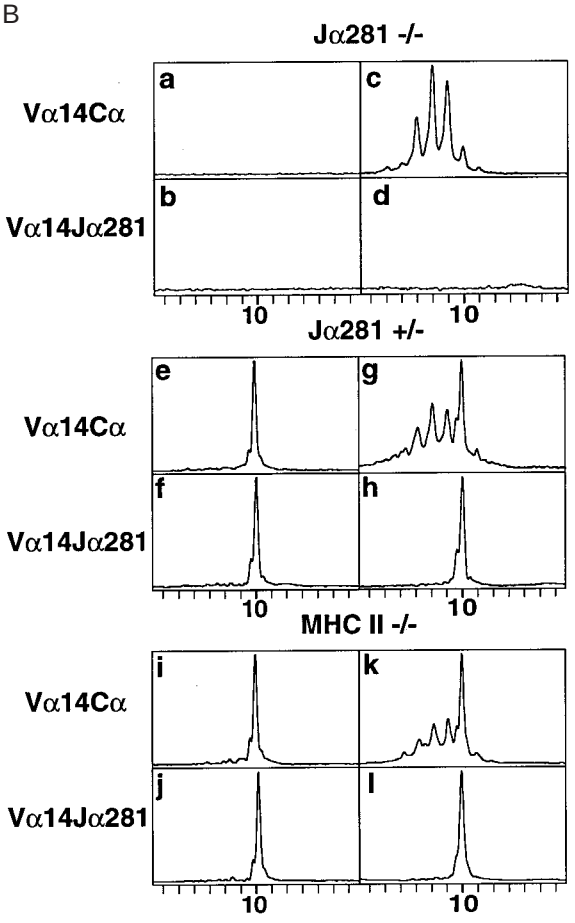


FIG. 2. The development of a sizable, granuloma-like structure depends on the recruitment of NKT cells. (*A*) Stained sections of the site of injection 7 days after injection of deproteinized cell walls in Jα281$^{-/-}$ mice [objectives: 2.5 (*a*), 6.3 (*b*), 40 (*c*), and oil, 100 (*d*)], Jα281$^{+/-}$ mice [2.5 (*e*), 6.3 (*f*), and 40 (*g*)], and C57BL/6 MHC class II$^{-/-}$ mice [2.5 (*h*), 6.3 (*i*), and 40 (*j*)]. (Bar = 1 mm.) (*B*) Vα14 and Vα14-Jα281 usages at the site of injection (*Left*) and in the lymph nodes (*Right*) of Jα281$^{-/-}$ (*a–d*), Jα281$^{+/-}$ (*e–h*), and C57BL/6 MHC class II$^{-/-}$ mice (*i–l*). The *x* and *y* axes are as in Fig. 1.

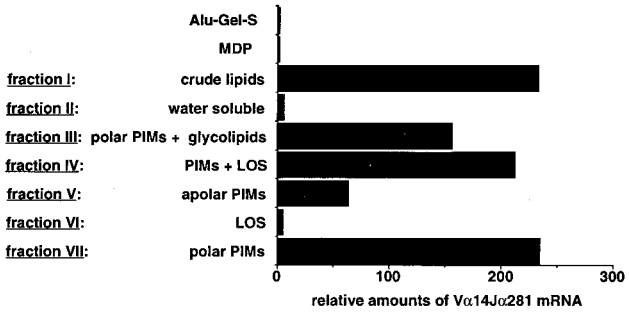


FIG. 3. Relative amounts of Vα14-Jα281 mRNA after immunization with Alu-Gel-S (0.25 mg), MDP (40 μg), crude mycobacterial lipids, and subsequent fractions prepared from them. The material contained in ≈10$^6$ bacteria was injected after adsorption onto Alu-Gel-S. The results (expressed as the ratio of the fluorescent PCR obtained by using Vα14Jα281 primers to fluorescent PCR signal obtained using hypoxanthine phosphoribosyltransferase primers) correspond to the average of results obtained in two animals.

Second, we examined the possible role of conventional CD4$^+$ T cells. In MHC-II$^{-/-}$ mice, which are deficient in CD4$^+$ conventional T cells but in which NKT cells differentiate normally, the injection of deproteinized mycobacterial cell walls led to the development at day 7 of the same lesions as in +/+ mice (Fig. 2*A*, *h–j*). The Vα14-Jα281 invariant TCRα chain was the only Vα14 chain detected in the lesions (Fig. 2*B*, *i* and *j*), and the Vα14-Cα and Vα14-Jα281 profiles of the lymph nodes of class II$^{-/-}$ mice were the same as in +/+ animals (Fig. 2*B*, *k* and *l*). The TCRβ repertoire of the cells present in the lesions of MHC-II$^{-/-}$ mice showed the same Vβ usage bias as C57BL/6$^{+/+}$ mice (data not shown). Also, mRNAs coding for the Igμ chain and for TCR γ/δ were detected as in C57BL/6$^{+/+}$ mice. Thus, highly organized, granuloma-like lesions containing the same cell types as in +/+ mice develop in the absence of CD4$^+$ T cells.

The absence of CD8-encoding mRNA ruled out a primary role for conventional CD8$^+$ T cells. Because CD1$^{-/-}$ mice were not available locally, the role of CD1 molecules in the granulomatous process was approached by injecting $\beta_2$m$^{-/-}$ mice, which are largely devoid of NKT cells. Large lesions developed, the lymphocyte content of which differed markedly from that of the lesions induced in +/+ mice: the mRNAs coding for the TCRβ and Vα14$^+$ chains as well as CD4, CD8, and IgMμ chains were not detectable in the lesions of $\beta_2$m$^{-/-}$ mice. By contrast, mRNAs coding for the TCR γ/δ chains were as in +/+ mice. The phenotypic changes resulting from disruption of the $\beta_2$m gene thus prevent the accumulation of B cells and α/β T cells in the lesions caused by deproteinized mycobacterial cell walls and also that of the rare NKT cells detectable in the lymph nodes of the same animals by using a clonotypic probe (data not shown).

**The NKT Cell-Recruiting Activity Is Associated to Mycobacterial Glycolipids, Particularly PIMs.** To identify the molecules responsible for the accumulation of NKT cells, the material was fractionated and the NKT cell recruiting activity of the different fractions was assayed *in vivo* by determining the relative amounts of NKT cells present at day 7 in the cell infiltrates recovered at the sites of injection. To avoid differences in the *in vivo* behavior of the injected molecules [for instance, differences in diffusion rate or in a specific internalization process (37)], the injected material was conjugated to

a neutral carrier, aluminium hydroxide (Alu-Gel-S; Serva), because C57BL/$6^{+/+}$ mice injected s.c. with particulate 0.25 mg Alu-Gel-S developed poor infiltrate with barely detectable V$\alpha$14-J$\alpha$281 mRNA (Fig. 3).

The crude lipids of H37 Rv cell walls (fraction I) adsorbed on Alu-Gel-S caused large, organized cell infiltrates with a core consisting of the carrier and neutrophils, surrounded by a thick rim of macrophages and lymphocytes. The formation of these structures also was found to depend on the presence of NKT cells, because they did not form in J$\alpha281^{-/-}$ mice (data not shown). In contrast to the structure caused by mycobacterial cell walls, the organized cell infiltrates induced by the crude glycolipids could be dissociated into living single cells, thus allowing the direct identification of NKT cells in the infiltrates by FACS analysis. Dead cells and macrophages were removed by Ficoll fractionation. Most of the $2.10^6$ living cells recovered from each granuloma were identified as neutrophils. All other cells were $CD45^+$ leukocytes (Fig. 4). No $CD19^+B220^+$ B cells were found. All $\alpha/\beta$ T lymphocytes were V$\alpha14^+$, TCR$\beta^{int}$, and $NK1.1^+$, thus, NKT cells. No $CD8^+$ and rare $CD4^+$ cells were detected. About 0.3% were non-NKT cells, and about 0.1% were $\gamma/\delta$ T cells (data not shown). RT-PCR analysis confirmed the absence of B cells and the presence of rearranged $\gamma/\delta$ TCR chains. Nearly all T cells in the infiltrates caused by crude lipids thus were $CD4^-CD8^-$ NKT cells.

The cells recruited by fraction I contained up to 200 times more V$\alpha$14-J$\alpha$281 mRNA than the cells recruited at the site of injection of Alu-Gel-S alone (Fig. 3). Although it is able to activate $\gamma/\delta$ T cells in man (23), the nonlipidic fraction (fraction II) was inefficient in recruiting NKT cells (Fig. 3). The immunoadjuvant muramyl-di-peptide (Sigma), a component of mycobacterial cell walls, yielded a cell infiltrate with no increase in the V$\alpha$14-J$\alpha$281 mRNA compared with Alu-Gel-S alone (Fig. 3). Fraction I was fractionated further, and the NKT cell-recruiting activity of the fractions was determined by RT-PCR. Nearly all the activity was recovered in the fractions containing PIMs (fractions III, IV, V, and VII) (Fig. 3), and the area of the V$\alpha$14-J$\alpha$281 peak was proportional to the amount of injected material. Upon analysis of the reactive fractions by TLC, the most active fractions were those containing highly polar PIMs, the structure of which was found compatible with tetra- to hexamannosylated PIMs ($PIM_{4-6}$) upon mass spectrometry analysis.

To determine whether NKT cells accumulated at random in the infiltrates induced by $PIM_{4-6}$, their TCR$\beta$ repertoire was determined by semiquantitative PCR and compared with the repertoire of liver NKT cells arbitrarily chosen as a representative of the peripheral NKT cells (38) (Fig. 5). Liver NKT cells

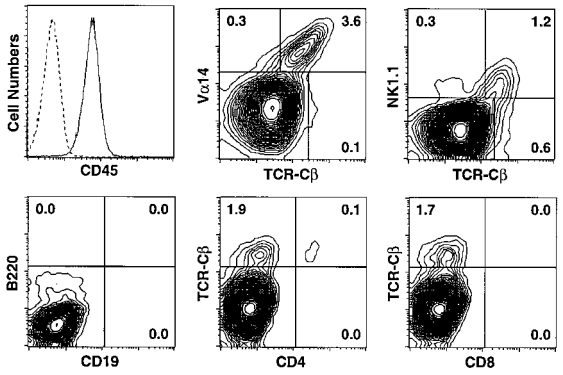


FIG. 4. FACS analysis of the cells recovered at the site of the s.c. injection of Alu-Gel-S/mycobacterial crude lipids in C57BL/6 mice. Depending on the experiments, the frequency of NKT cells varies from 1.7 to 3.6% of total cells recovered after Ficoll fractionation. The dotted line in the histogram corresponds to unstained cells.

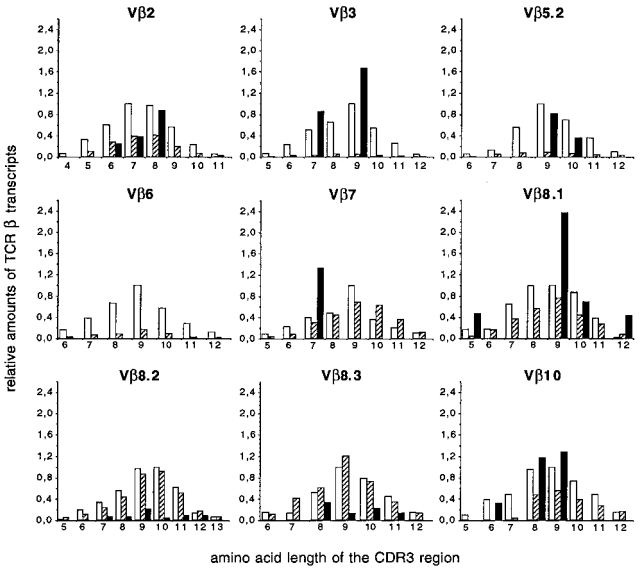


FIG. 5. Semiquantitative analysis of the TCR$\beta$ chain repertoire of NKT cells isolated from the liver of control mice (hatched bars) and recruited by $PIM_{4-6}$ (solid bars), and of lymph node T cells, used here as the internal control for primer efficiency (open bars). The value "1" is attributed arbitrarily to the area of highest peak of the Gaussian pattern obtained from the lymph node T cells. Only the most represented families of V$\beta$-C$\beta$ in granuloma-like structures have been studied by semiquantitative PCR analysis. V$\beta$6, absent from granuloma-like structures, was used as a negative control.

were confirmed to have a V$\beta$ usage skewed toward V$\beta$8 and V$\beta$7 compared with conventional T cells. Each family of V$\beta$-C$\beta$ rearrangements showed a Gaussian CDR3-length distribution indicative of a diverse, polyclonal TCR$\beta$ repertoire. By contrast, the NKT cells present in the infiltrate caused by the injection of $PIM_{4-6}$ showed a differently skewed V$\beta$ usage (Fig. 5). In addition, distinctive rearrangements [such as the V$\beta$8.1-C$\beta$ rearrangement(s) with a 9-aa length CDR3 in Fig. 5], found in large excess compared with the Gaussian distribution of the controls, were indicative of an oligoclonal distribution of NKT cells in the infiltrates. All injected mice studied showed the same skewing of the V$\beta$ usage, however, with a variable length of CDR3 regions among animals.

## DISCUSSION

The formation of granulomas is an early immune response of the host, which is viewed as contributing to preventing the dissemination of some pathogens. The complex cellular and molecular mechanisms that underlie the formation of granulomas are not fully understood, although they involve different cell types and cytokines such as IFN-$\gamma$ and IL-12 (39, 40). In earlier studies of the steps of the granulomatous response to microbial components in the absence of bacterial proliferation, the injection of deproteinized bacterial cell wall, which leads to the formation of granuloma-like structures, has been largely used (reviewed in refs. 41 and 42). We have used a similar approach to identify the T cells involved in the early response to nonpeptidic, mycobacterial cell wall components. We have found that NKT cells are detected at the earliest stages of the granulomatous response and that they play a primary role in the processes leading to the granulomatous response to deproteinized mycobacterial cell walls. Finally, the accumulation of NKT cells is associated with the presence of mycobacterial oligomannosylated GPI, particularly, PIMs. These results provide new insights into the contribution of NKT cells to the early response of a host against pathogens.

The way NKT cells contribute to the granulomatous response is still unclear. We have shown that the cells do not infiltrate randomly the site of injection. This could have been achieved through the activation of the cells by properly presented antigens, in the present case by glycolipids presented by CD1 to the TCR of the NKT cells. Because the present study was carried out *in vivo*, the role of CD1d in the *in vivo* presentation of PIMs to NKT cells could not be investigated directly. Despite the fact that, *in vitro*, unprimed NKT cells could not be activated by synthetic $PIM_2$ (which may differ slightly from the natural $PIM_2$ and from $PIM_{4-6}$) presented by the CD1 molecules (8), all evidence points to the ability of CD1 to bind a large variety of glycolipids including PIMs (6, 7, 10, 31, 32, 34–36, 43). So far, molecules with the proper fatty acid tails bind to CD1, and their hydrophilic moiety governs T cell recognition: synthetic ceramides bound to human or to murine CD1d molecules are recognized through their carbohydrate moiety by the TCR of NKT cell hybridomas, and the recognition requires the expression of the V$\alpha$14-invariant TCR$\alpha$ chain and depends on the TCR$\beta$ chain expressed (6, 8, 9). The oligoclonality of the NKT cells in $PIM_{4-6}$-induced infiltrates is consistent with a selection of the cells by the carbohydrate moiety of the PIMs.

Conversely, it can be argued that the infiltrating NKT cells are activated in a CD1-independent manner and their activation may be caused directly by glycolipids. For example, the lectin-like structures or other receptors common to NK and NKT cells may directly recognize the carbohydrate moiety of glycolipids, with no presentation step, and their cross-linking could result in the activation of the cells. This might explain why an ambiguous, local response develops in injected $\beta_2m^{-/-}$ mice, in which the activity of NK cells is likely to be disregulated because of the absence of MHC class I molecules**.**

The organ(s) from which the granuloma NKT cells are recruited is not known. Because little is known of the properties of the NKT cells in the different organs, one may hypothesize that the infiltrating NKT cells originate from a compartment in which they are already oligoclonal.

These different types of recruiting/activating mechanisms also may cooperate in the recruitment of NKT cells by glycolipids, which is part of the early response of the host to nonpeptide mycobacterial components. The system we have used should serve as a powerful tool to study *in vivo* the induction of NKT cell responses and, thereby, their role in immunopathology.

I.A. acknowledges receipt of Institut National de la Santé et de la Recherche Médicale/Japan Society for the Promotion of Science and Ministère de la Recherche et de l'Espace fellowships. This work has been supported by the "axe Immunologie des tumeurs" of La Ligue contre le Cancer, European Economic Community, the Institut National de la Santé et de la Recherche Médicale, Institut Pasteur, Tsukuba University, Presto Research Projects, and the Japanese Ministry of Education.

1. Bendelac, A., Lantz, O., Quimby, M. E., Yewdell, J. W., Bennink, J. R. & Brutkiewicz, R. R. (1995) *Science* **268,** 863–865.
2. Ortaldo, J. R., Winckler-Pickett, R., Mason, A. T. & Mason, L. H. (1998) *J. Immunol.* **160,** 1158–1165.
3. Koseki, H., Asano, H., Inaba, T., Miyashita, N., Moriwaki, K., Lindahl, K. F., Mizutani, Y., Imai, K. & Taniguchi, M. (1991) *Proc. Natl. Acad. Sci. USA* **88,** 7518–7522.
4. Lantz, O. & Bendelac, A. (1994) *J. Exp. Med.* **180,** 1097–1106.
5. Bendelac, A., Rivera, M. N., Park, S. H. & Roark, J. H. (1997) *Annu. Rev. Immunol.* **15,** 535–562.
6. Brossay, L., Naidenko, O., Burdin, N., Matsuda, J., Sakai, T. & Kronenberg, M. (1998) *J. Immunol.* **161,** 5124–5128.
7. Kawano, T., Cui, J., Koezuka, Y., Toura, I., Kaneko, Y., Motoki, K., Ueno, H., Nakagawa, R., Sato, H., Kondo, E., *et al.* (1997) *Science* **278,** 1626–1629.
8. Burdin, N., Brossay, L., Koezuka, Y., Smiley, S. T., Grusby, M. J., Gui, M., Taniguchi, M., Hayakawa, K. & Kronenberg, M. (1998) *J. Immunol.* **161,** 3271–3281.
9. Brossay, L., Chioda, M., Burdin, N., Koezuka, Y., Casorati, G., Dellabona, P. & Kronenberg, M. (1998) *J. Exp. Med.* **188,** 1521–1528.
10. Schofield, L., McConville, M. J., Hansen, D., Campbell, A. S., Fraser-Reid, B., Grusby, M. J. & Tachado, S. D. (1999) *Science* **283,** 225–229.
11. Takeda, K., Seki, S., Ogasawara, K., Anzai, R., Hashimoto, W., Sugiura, K., Takahashi, M., Satoh, M. & Kumagai, K. (1996) *J. Immunol.* **156,** 3366–3373.
12. Cui, J., Shin, T., Kawano, T., Sato, H., Kondo, E., Toura, I., Kaneko, Y., Koseki, H., Kanno, M. & Taniguchi, M. (1997) *Science* **278,** 1623–1626.
13. Kawano, T., Cui, J., Koezuka, Y., Toura, I., Kaneko, Y., Sato, H., Kondo, E., Harada, M., Koseki, H., Nakayama, T., *et al.* (1998) *Proc. Natl. Acad. Sci. USA* **95,** 5690–5693.
14. Hammond, K. J. L., Poulton, L. D., Palmisano, L. J., Silveira, P. A., Godfrey, D. I. & Baxter, A. G. (1998) *J. Exp. Med.* **187,** 1047–1056.
15. Flesch, I. E. A., Wandersee, A. & Kaufmann, S. H. E. (1997) *J. Immunol.* **159,** 7–10.
16. Enomoto, A., Nishimura, H. & Yoshikai, Y. (1997) *J. Immunol.* **158,** 2268–2277.
17. Mieza, M. A., Itoh, T., Cui, J. Q., Makino, Y., Kawano, T., Tsuchida, K., Koike, T., Shirai, T., Yagita, H., Matsuzawa, A., *et al.* (1996) *J. Immunol.* **156,** 4035–4040.
18. Wilson, S. B., Kent, S. C., Patton, K. T., Orban, T., Jackson, R. A., Exley, M., Porcelli, S., Schatz, D. A., Atkinson, M. A., Balk, S. P., *et al.* (1998) *Nature (London)* **391,** 177–181.
19. Emoto, M., Emoto, Y. & Kaufmann, S. H. (1997) *Eur. J. Immunol.* **27,** 183–188.
20. Emoto, Y., Emoto, M. & Kaufmann, S. H. (1997) *Infect. Immun.* **65,** 5003–5009.
21. Cosgrove, D., Gray, D., Dierich, A., Kaufman, J., Lemeur, M., Benoist, C. & Mathis, D. (1991) *Cell* **66,** 1051–1066.
22. Koller, B. H., Marrack, P., Kappler, J. W. & Smithies, O. (1990) *Science* **248,** 1227–1230.
23. Constant, P., Davodeau, F., Peyrat, M.-A., Poquet, Y., Puzo, G., Bonneville, M. & Fournié, J.-J. (1994) *Science* **264,** 267–270.
24. Regnault, A., Levraud, J. P., Lim, A., Six, A., Moreau, C., Cumano, A. & Kourilsky, P. (1996) *Eur. J. Immunol.* **26,** 914–921.
25. Pannetier, C., Cochet, M., Darche, S., Casrouge, S., Zöller, M. & Kourilsky, P. (1993) *Proc. Natl. Acad. Sci. USA* **90,** 4319–4323.
26. Azuara, V., Levraud, J. P., Lembezat, M. P. & Pereira, P. (1997) *Eur. J. Immunol.* **27,** 544–553.
27. Pannetier, C., Levraud, J.-P., Lim, A., Even, J. & Kourilsky, P. (1997) in *The T-Cell Receptor: Selected Protocols and Applications,* eds. Okseznberg, J. R., Wang, L. & Jeffery, J.-Y. Y. (Chapman & Hall, New York), pp. 287–324.
28. Cibotti, R., Cabaniols, J. P., Pannetier, C., Delarbre, C., Vergnon, I., Kanellopoulos, J. M. & Kourilsky, P. (1994) *J. Exp. Med.* **180,** 861–872.
29. Levraud, J. P., Pannetier, C., Langlade-Demoyen, P., Brichard, V. & Kourilsky, P. (1996) *J. Exp. Med.* **183,** 439–449.
30. Masuda, K., Makino, Y., Cui, J., Ito, T., Tokuhisa, T., Takahama, Y., Koseki, H., Tsuchida, K., Koike, T., Moriya, H., *et al.* (1997) *J. Immunol.* **158,** 2076–2082.
31. Beckman, E. M., Porcelli, S. A., Morita, C. T., Behar, S. M., Furlong, S. T. & Brenner, M. B. (1994) *Nature (London)* **372,** 691–694.
32. Sieling, P. A., Chatterjee, D., Porcelli, S. A., Prigozy, T. I., Mazzaccaro, R. J., Soriano, T., Bloom, B. R., Brenner, M. B., Kronenberg, M., Brennan, P. J. *et al.* (1995) *Science* **269,** 227–230.
33. Beckman, E. M., Melian, A., Behar, S. M., Sieling, P. A., Chatterjee, D., Furlong, S. T., Matsumoto, R., Rosat, J. P., Modlin, R. L. & Porcelli, S. A. (1996) *J. Immunol.* **157,** 2795–2803.
34. Exley, M., Garcia, J., Balk, S. P. & Porcelli, S. (1997) *J. Exp. Med.* **186,** 109–120.
35. Moody, D. B., Reinhold, B. B., Guy, M. R., Beckman, E. M., Frederique, D. E., Furlong, S. T., Ye, S., Reinhold, V. N., Sieling, P. A., Modlin, R. L., *et al.* (1997) *Science* **278,** 283–286.
36. Spada, F. M., Koezuka, Y. & Porcelli, S. A. (1998) *J. Exp. Med.* **188,** 1529–1534.
37. Prigozy, T. I., Sieling, P. A., Clemens, D., Stewart, P. L., Behar, S. M., Porcelli, S. A., Brenner, M. B., Modlin, R. L. & Kronenberg, M. (1997) *Immunity* **6,** 187–197.
38. Watanabe, H., Miyaji, C., Kawachi, Y., Iiai, T., Ohtsuka, K., Iwanage, T., Takahashi-Iwanaga, H. & Abo, T. (1995) *J. Immunol.* **155,** 2972–2983.
39. de Jong, R., Altare, F., Haagen, I. A., Elferink, D. G., Boer, T., van Breda Vriesman, P. J., Kabel, P. J., Draaisma, J. M., van Dissel, J. T., Kroon, F. P., *et al.* (1998) *Science* **280,** 1435–1438.
40. Altare, F., Durandy, A., Lammas, D., Emile, J.-F., Lamhamedi, S., Le Deist, F., Drysdale, P., Jouanguy, E., Döffinger, R., Bernaudin, F., *et al.* (1998) *Science* **280,** 1432–1432.
41. Warren, K. S. (1976) *Ann. N. Y. Acad. Sci.* **278,** 7–18.
42. Majno, G. & Joris, I. (1996) *B. Science Cambridge* (Oxford Univ. Press, Oxford), pp. 974–981.
43. Joyce, S., Woods, A. S., Yewdell, J. W., Bennink, J. R., De, S. A., Boesteanu, A., Balk, S. P., Cotter, R. J. & Brutkiewicz, R. R. (1998) *Science* **279,** 1541–1544.